Journal of Marine Science and Technology

Volume 31 | Issue 4 Article 9

An MRF Model-based Study on the Effect of Fishes upon the Characteristics of Flow Field of an Aquaculture Tank

Xian-ying Shi
College of Ocean and Civil Engineering, Dalian Ocean University, Dalian, China

Zheng-zheng Huang
College of Ocean and Civil Engineering, Dalian Ocean University, Dalian, China

Meng Li
College of Ocean and Civil Engineering, Dalian Ocean University, Dalian, China

Yinxin Zhou
Key Laboratory of Environment Controlled Aquaculture (Dalian Ocean University) Ministry of Education, China;

Xiao-zhong REN
Key Laboratory of Environment Controlled Aquaculture (Dalian Ocean University) Ministry of Education, China

See next page for additional authors

An MRF Model-based Study on the Effect of Fishes upon the Characteristics of Flow Field of an Aquaculture Tank

Authors

Xian-ying Shi, Zheng-zheng Huang, Meng Li, Yinxin Zhou, Xiao-zhong REN, Hang-fei LIU, and Shu-peng Du

RESEARCH ARTICLE

An MRF Model-based Study on the Effect of Fishes upon the Characteristics of Flow Field of an Aquaculture Tank

Xian-Ying Shi [a,b], Zheng-Zheng Huang [a,b], Meng Li [a,b], Yinxin Zhou [b,c], Xiao-Zhong Ren [b,c,*], Hang-Fei Liu [d,**], Shu-Peng Du [b,c]

[a] College of Ocean and Civil Engineering, Dalian Ocean University, Dalian, China
[b] Key Laboratory of Environment Controlled Aquaculture (Dalian Ocean University) Ministry of Education, China
[c] College of Marine Technology and Environment, Dalian Ocean University, Dalian, China
[d] College of Biosystems Engineering and Food Science, Zhejiang University, Zhejiang, China

Abstract

The study aims to investigate the effect of fish movement on the flow field in the aquaculture tank of a recirculating water aquaculture system. Herein, based on the Navier−Stokes equations and the RNG k-ϵ turbulence model, the flow field in the aquaculture tank with fish movement was numerically simulated using the multiple reference frame (MRF) model and compared with the numerical simulation results of the fishless aquaculture tank. The results revealed that the overall mean flow velocity in the tank decreased significantly when the fish swam counter-currently with a fixed trajectory, and the overall mean flow velocity increased slightly when the number of fish increased. When the same number of fish swam counter-currently with a fixed trajectory, the effect of side-by-side distribution on the overall mean flow velocity in the tank was slightly greater than that of the back-and-forth and top-and-bottom distributions. Under the influence of fish counter-current swimming, the flow field uniformity in the aquaculture tank was significantly reduced, the turbulence intensity increased, the flow velocity at the tank wall increased, and the low-flow velocity area appeared in the center of the tank. The study demonstrated the necessity of considering the impact of fish counter-current swimming on the flow field within an aquaculture tank. This consideration is crucial when seeking to raise fish welfare, improve production operation management and optimize the structure of the aquaculture tank.

Keywords: MRF model, Fish, Numerical simulation, Flow field

1. Introduction

The recirculating aquaculture system (RAS) is a new aquaculture model that saves resources and environmental protection, is productive with low consumption [1−4], and allows the flow field conditions in the tank to be "customized" to the fish needs. The RAS refers to using advanced equipment to control the aquaculture environment and provide an optimal living environment for the fish [5]. The aquaculture environment is controlled by advanced equipment to provide the best possible environment for the fish.

The characteristics of the flow field in an aquaculture tank affect residual bait and feces settlement and discharge, ammonia nitrogen distribution, and dissolved oxygen and directly affect fish survival and their behavioral activities [6]. The right flow rate in an aquaculture tank changes the fish growth rate by affecting energy consumption and improving their quality [7]. Simultaneously, increasing the flow rate can effectively improve the scouring of fish surface by the water, which has a beneficial effect on

Received 30 June 2023; revised 19 October 2023; accepted 31 October 2023.
Available online 15 December 2023

* Corresponding author. Key Laboratory of Environment Controlled Aquaculture (Dalian Ocean University) Ministry of Education, China.

** Corresponding author.
E-mail addresses: renxiaozhong@dlou.edu.cn (X.-Z. Ren), liuhangfei@zju.edu.cn (H.-F. Liu).

https://doi.org/10.51400/2709-6998.2716

preventing fish diseases. Determining flow field characteristics after tank stabilization is crucial for its design and layout. A homogeneous and stable flow field will provide a better living space for the aquaculture organisms, improve the circulation effect of the tank, and save operating costs.

The aquaculture equipment size in a planted aquaculture system is usually large, and the existing studies on the hydrodynamic characteristics of aquaculture tanks are mainly based on model tests.

Introducing computational fluid dynamic (CFD) numerical simulation methods allows for quickly building a farm tank model and calculating the flow field data, substantially reducing the research period. The numerical simulation method enables obtaining the tank hydrodynamic characteristics at any point, allowing the flow field to be "visualized".

Masaló, I [8] researched about the influence of fish swimming on the flow pattern of circular tanks, and discovered that fish can drag down the average flow velocity of the aquaculture tanks. It was also discovered that smaller fish drag more velocity when in same culture density. Masaló, I [9] and Plew [10] discovered that the turbulence intensity caused by fish swimming activities is positively correlated with stocking density by conducting actual experiments. LIU [11] conducted a study on the correlation between fish movements and flow fields using the computational fluid dynamics (CFD) method. The impact of culture tanks equipped with a Cornell-type dual-drain system on turbulence intensity and velocity fields was investigated by Gorle [12,13] and Zhang [14], Leila Behrooz [15] used CFD methods to study the turbulence properties of circular aquaculture tanks in different diameters. ZHANG [16] proposed a method of optimization of aquaculture tank physical parameters based on computational fluid mechanics (CFD) and machine learning (ML). Boris Miguel López-Rebollar [17] adopted physical experiment and CFD simulation on researching particle sedimentation efficiency. The numerical simulation of unloaded aquaculture tanks using CFD methods has been conducted in several studies by A. Lunger, Liu Naishuo, and AN [18−20]. Suggestions have been made to improve the aquaculture tank shape and inlet and outlet facilities.

Most domestic studies on the hydrodynamic characteristics of aquaculture tanks neglect the influence of aquaculture organisms on the flow field characteristics. Plew et al. [10] studied the changes in flow velocity and turbulence caused by different stocking fish densities in a circular aquaculture tank using real measurements, showing that fish swimming in the aquaculture tank significantly reduced the flow velocity. Liu, Haibo [21] established a three-dimensional numerical calculation model of the mutual coupling between the farmed fish model and the farmed flow field using *Sebastes schlegelii* as the research object and simulated the effect of shedding vortex formed by the fish swinging their tails on the flow field characteristics of farmed tank.

We introduced the multiple reference frame (MRF) into a three-dimensional turbulence numerical calculation model based on CFD technology to combine the fish and fluid motion of an aquaculture tank to realize fish swimming behavior simulation on an aquaculture tank according to a fixed trajectory. This paper compares the flow field characteristics of an unloaded aquaculture tank with those of a fish-containing tank to reveal the effect of fish movement in an aquaculture tank on the flow field characteristics according to a fixed trajectory.

2. Numerical modeling

2.1. Numerical model theory

Turbulence exists in the fluid movement in aquaculture tanks and should be considered when constructing numerical models for aquaculture tanks. The RNG k-ϵ model is more suitable than the standard k-ϵ model for simulating flow characteristics in aquaculture tanks due to the better handling of flows with high strain rates and greater flow curvature [22].

The three-dimensional N−S equations were solved by the finite volume method, the NG k-ϵ turbulence model equations were solved by the finite difference method, the pressure implicit solution was used, the SIMPLE algorithm was used for pressure−velocity coupling, and the turbulent kinetic energy was in the first-order windward discrete format. The continuity and Reynolds-averaged N−S equations are expressed as follows:

Continuity equation:

$$\frac{\partial \rho}{\partial t}+\frac{\partial(\rho u)}{\partial x}+\frac{\partial(\rho v)}{\partial y}+\frac{\partial(\rho w)}{\partial z}=0 \tag{1}$$

N−S equation:

$$X-\frac{1}{\rho}\frac{\partial p}{\partial x}+\frac{\mu}{\rho}\nabla^2 u_x=\frac{\partial u_x}{\partial t}+u_x\frac{\partial u_x}{\partial x}+u_y\frac{\partial u_x}{\partial y}+u_z\frac{\partial u_x}{\partial z} \tag{2}$$

$$Y-\frac{1}{\rho}\frac{\partial p}{\partial y}+\frac{\mu}{\rho}\nabla^2 u_y=\frac{\partial u_y}{\partial t}+u_x\frac{\partial u_y}{\partial x}+u_y\frac{\partial u_y}{\partial y}+u_z\frac{\partial u_y}{\partial z} \tag{3}$$

$$Z-\frac{1}{\rho}\frac{\partial p}{\partial z}+\frac{\mu}{\rho}\nabla^2 u_z=\frac{\partial u_z}{\partial t}+u_x\frac{\partial u_z}{\partial x}+u_y\frac{\partial u_z}{\partial y}+u_z\frac{\partial u_z}{\partial z} \tag{4}$$

where X, Y, and Z are the unit mass force components per unit mass of fluid; $\frac{1}{\rho}\frac{\partial p}{\partial x}$, $\frac{1}{\rho}\frac{\partial p}{\partial y}$, and $\frac{1}{\rho}\frac{\partial p}{\partial z}$ are the normal stress components per unit mass of fluid; and $\frac{\mu}{\rho}\nabla^2 u_x$, $\frac{\mu}{\rho}\nabla^2 u_y$, and $\frac{\mu}{\rho}\nabla^2 u_z$ are the tangential stress components per unit mass of fluid.

The transport equation for the RNG k-ϵ model is as follows:

Turbulent kinetic energy k equation:

$$\frac{\partial(\rho k)}{\partial t}+\frac{\partial(\rho u_i k)}{\partial x_i}=\frac{\partial}{\partial x_j}\left[\partial_k(\mu+\mu_t)\frac{\partial k}{\partial x_j}\right]+G_k-\rho\epsilon \tag{5}$$

Turbulent kinetic energy dissipation rate ϵ equation:

$$\frac{\partial(\rho\epsilon)}{\partial t}+\frac{\partial(\rho u_i\epsilon)}{\partial x_i}=\frac{\partial}{\partial x_j}\left[\alpha_\epsilon(\mu+\mu_t)\frac{\partial\epsilon}{\partial x_j}\right]+\frac{\epsilon}{k}(C_{1\epsilon}G_k-C_{2\epsilon}\rho\epsilon) \tag{6}$$

where ρ is the density of fluid; μ_t is the vortex cluster viscosity coefficient; G_k is the turbulent kinetic energy due to the mean velocity gradient; and α_ϵ is the inverse of the effective Planck number of ϵ.

$$\mu_t=C_\mu\frac{k^2}{\epsilon} \tag{7}$$

$$G_k=\mu_t\left(\frac{\partial u_i}{\partial x_j}+\frac{\partial u_j}{\partial x_i}\right)\frac{\partial u_i}{\partial x_j} \tag{8}$$

The relevant parameters are as follows: $C_{1\epsilon}=1.42$, $C_{2\epsilon}=1.68$, $C_\mu=0.0845$, and $\alpha_k=\alpha_\epsilon=1.39$.

2.2. MRF model

Due to the presence of fish in the farm tank, the mesh was encrypted to generate many meshes and a dynamic mesh model technique was required. Each sub-domain could be set to move independently, stationary, rotating, or translating. The MRF model simulated the fish movement in a tank by setting the sub-domain where the fish were located as a rotational region and the rest as a stationary region. The flow field control equations were solved in each sub-domain, and the flow field information was exchanged at the sub-domain intersection by converting the velocity to absolute velocity. The MRF model also reduced the computational effort and time required to simulate fish movement in the tank and was particularly advantageous for simulating fish movement. Therefore, the MRF model was used in this paper to perform simulations.

2.3. Aquaculture tank model build

The diameter of the breeding tank was 1 m, the depth of water was 20 cm, and the bottom of the tank was horizontal. Two inlet pipes with a pipe diameter of 2 cm were used, and each inlet pipe was evenly opened with nine holes with a hole diameter of 4 mm, which were laid at a distance of 2 cm from the tank wall. The water flow rate in and out of the two tanks was equal, set to 0.814 m^3/h, the inlet velocity $V_{in}=1$ m/s, and the outlet was set in the center of the tank bottom, with a diameter of 0.02 m. The sub-domain of the fish model trajectory was set to be a rotating region in the tank model (Sub-domain within blue framework), and the rest of the region was set to be a static region (Fig. 1).

2.4. Meshing and irrelevance verification

This study used the dynamic mesh modeling technique. The main body of the aquaculture tank meshed with the hexahedral mesh delineation technique, the surface of the fish model, and the water inlet were meshed with tetrahedral mesh, and mesh encryption was conducted, and Fig. 2 depicts the mesh delineation.

Three grid levels (H/M/L) were used to calculate the overall mean flow velocity within the aquaculture tank for grid-independent verification to reduce the calculation time cost and improve the calculation efficiency. Table 1 presents the grid numbers and calculation results, illustrating that the difference between the overall mean flow velocity within the medium- and the higher-density grid aquaculture tanks was insignificant. In contrast, the overall mean flow velocity within the low-density grid aquaculture tank was significantly higher than the calculated results of the other two grid quantities. Figure 3 illustrates a comparison of the overall mean flow velocity in the tank for the three grid quantities with different iteration steps, revealing a little difference between the medium- (M) and the high-density grids (H) in the overall mean flow velocity at different iteration steps. Therefore, the

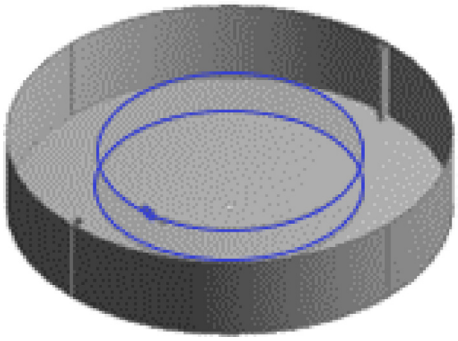

Fig. 1. The diagrammatic sketch of the tank model with the presence of fish.

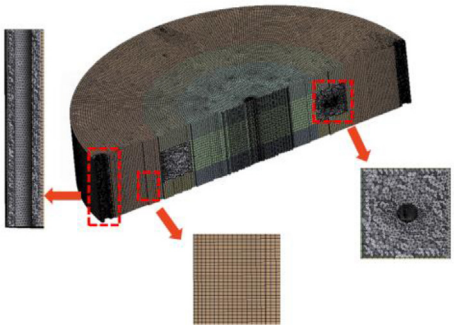

Fig. 2. The diagrammatic sketch of mesh division.

Table 1. Comparison of the calculated results for the different numbers of grids.

Level of mesh	Number of grids	Number of nodes	Average velocity (V_{age}, m/s)
H (high)	3624042	2656477	0.0897 m/s
M (medium)	3111433	544768	0.0874 m/s
L (low)	1838140	325166	0.0971 m/s

medium-density grid was chosen for the numerical simulation.

2.5. Initial boundary conditions

In the numerical calculation process, the internal moving region (fwater) was set to rotate at the same speed as the internal cylindrical region. The external sub-domain was stationary, the external cylindrical surface and the lower bottom surface were set to the stationary wall boundary condition (stationary wall), the farmed fish model was set to the moving wall boundary condition (moving wall), the region where the farmed fish was located. The fish were situated in a region characterized by limited movement, as were the surrounding areas. The interface between the individuals and their immediate surroundings was primarily confined to the interior surface area. The inlet boundary was set as a velocity inlet with an inlet velocity of 1 m/s. The flow velocity was uniformly distributed, and the turbulence intensity was 5.7 %. The hydraulic diameter was established to be 0.004 m, and the pressure value was set to standard atmospheric pressure The outlet boundary condition was defined as free outflow, and the bottom flow divergence ratio was set to 1.

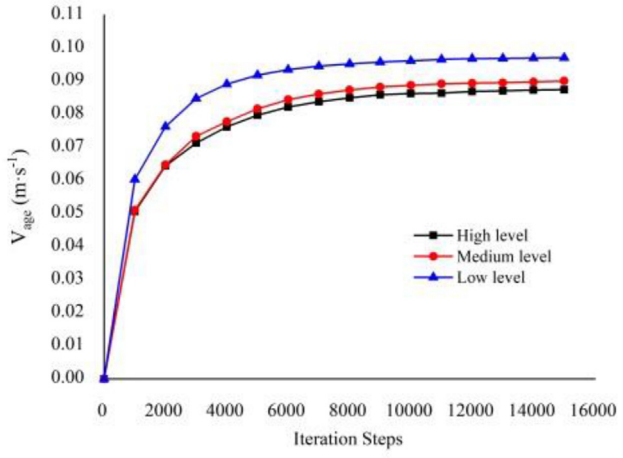

Fig. 3. Comparison of the calculated results from three different numbers of grids.

The residuals were set for the model monitor, the residuals convergence value was set to 10^{-4}, the values were initialized for all zones, and finally, the number of iteration steps was set to 16000. The residual curve convergence was monitored at each step to see if the set residuals were reached. After the model had converged, the results were obtained, and the calculated data were saved [23].

2.6. Fish model build

The redfin puffer was used as the simulation object of *Takifugu rubripes*. Except for predation and avoidance of danger, the redfin puffer mostly swims with its caudal and pectoral fins not oscillating and its body nearly gliding. Considering this swimming characteristic, the body of the redfin puffer was simplified into a rigid body model without fins, and the curvature of the body was set according to the trajectory of movement (Fig. 4). The length of the fish model was 90 mm, and the width was 27 mm.

2.7. Model validation

We verified the accuracy of the numerical modeling of a physical model test tank based on Masaló, I [8]. The tank diameter was 1.44 m, and the water depth was 30 cm. An inlet pipe with a diameter of 50 mm was used, which opened to a 20.5 mm diameter inlet at 15 cm from the tank bottom. Moreover, the jet direction was tangent to the tank wall, with a jet velocity of 1.27 m/s (the flow rate of Q = 1500 L/h). The outlet was located at the bottom of the tank center, with a 75 mm riser in the tank center and a hole at the bottom of the riser connected to the outlet at the tank bottom. A 75 mm vertical pipe in the tank center was connected to the outlet at the tank bottom by a hole at the bottom of the vertical pipe. The tank was stocked with 49 fish (individual length of 22.5 cm and weight of 153.9 g) at a stocking density of 14.62 kg/m^3. Figure 5 displays the tank model.

The same flow rate monitoring points were set in the numerical model as in the model test. The flow

a) Photograph of *Takifugu rubripes*.

b) Front view. c) Vertical view. d) Cubic diagram.

Fig. 4. The diagrammatic sketch of Takifugu rubripes.

rate values of each monitoring point were extracted after the numerical model was stable. The comparison between the numerically calculated flow rate values of each monitoring point and Fig. 6 presents the measured values of the model test, illustrating that the numerically calculated values match well with the measured model test values. Consequently, the constructed mathematical model can be used to study the flow field characteristics of the fish culture tank.

3. Results and discussion

3.1. Influence of aquaculture fish on the overall mean flow rate of aquaculture tank

We investigated the effect of the swimming behavior of fish in a fixed trajectory (15 cm from the bottom of the tank and 25 cm from the vertical line in the center) against the current on the overall mean flow velocity in the aquaculture tank under two condition types (different numbers (Fig. 7) and spatial distribution of the fish (Fig. 8)), which was

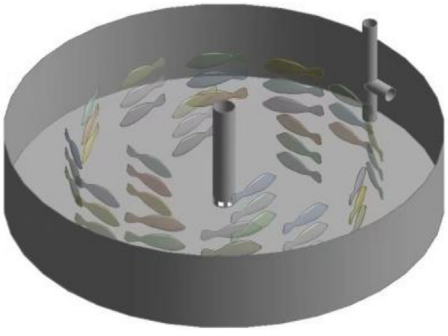

Fig. 5. Physical examination model tank adopted by Masaló, I.

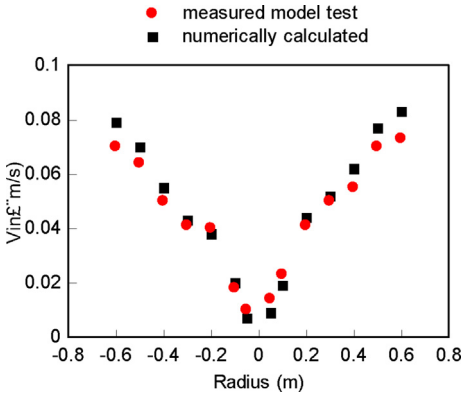

Fig. 6. Comparison of flow velocity between physical experiment and numerical calculation results.

then compared with that of the overall mean flow velocity in the unloaded aquaculture tank. Table 2 shows the overall mean flow velocities in the tanks under various conditions (due to the small differences in flow velocities between conditions, the flow velocities have been retained to four significant digits).

Table 2 demonstrates that the tank velocities all decreased when different numbers of fish swam counter-currently in fixed trajectories compared with the overall mean velocity in the fishless tank. The magnitude of the decline had a positive correlation to the number of fish but with a negligible variation in magnitude. Specifically, the smallest reduction was 15.4 %, while the highest was 16.9 %.

Table 2 depicts that when fish were distributed in different spatial ways and swam counter-currently with a fixed trajectory, the overall mean flow velocity in the aquaculture tank decreased by 14.9 %−15.7 %

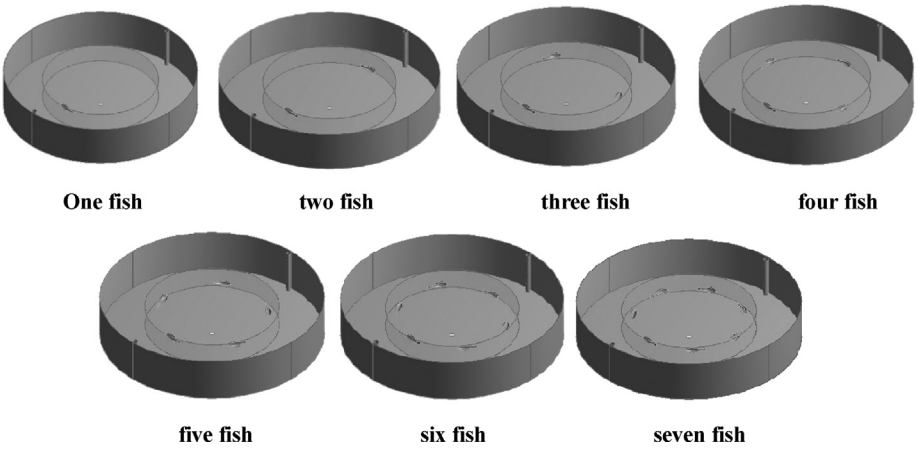

Fig. 7. Model illustration.

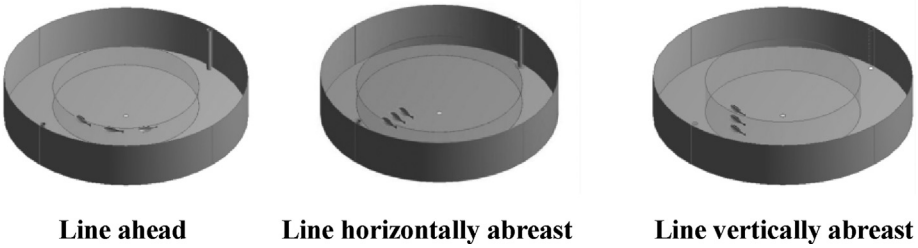

Fig. 8. Model illustration.

Table 2. The overall average speed in the aquaculture tank under different working conditions.

Case	Number of fish	Average velocity	Rate of change
No Fish	0	0.1043	–
	1	0.0877	15.9
Quantity Variation	2	0.0879	15.7
	3	0.0882	15.4
	4	0.0876	16.0
	5	0.0873	16.3
	6	0.0871	16.5
	7	0.0867	16.9
Spatial Distribution	3	0.0888	14.9
	3	0.0879	15.7
	3	0.0887	15.0

from the overall mean flow velocity in the unloaded tank, with a slightly larger decrease in the side-by-side mode, and not much difference in the longitudinal and up-and-down distribution of the fish.

Accordingly, the flow velocity maps of a horizontal cross-section of 15 cm from the tank bottom with a fish moving in a fixed trajectory in the fish culture tank were compared with those of the unloaded tank (Fig. 9). Figure 9 demonstrates that the decrease in the general average flow velocity in the tank was insignificant. Consequently, the flow velocity distribution in the other areas remained insignificantly unchanged, except for the central region of the fish culture tank, where a significantly low flow velocity region emerged. Extracting the flow velocity values in one diameter on a horizontal cross-section 15 cm from the bottom of the tank for comparison between the two conditions (Fig. 10) showed that the flow velocities were reduced in most corresponding points in the fish aquaculture tanks compared with the unloaded tanks. However, the flow velocities in the side walls of tanks were higher than in the unloaded condition.

3.2. Influence of fish motion on flow field uniformity in the aquaculture tank

This study quantitatively assesses the effect of fish activity on the uniformity of the flow field in an aquaculture tank using the parameters UC_{50} [24] and DU_{50} [25,26]:

$$UC_{50} = \frac{V_{L50}}{V_{H50}} \tag{9}$$

where UC_{50} is the uniformity factor of the breeding tank; VL_{50} is the average value of velocity for 50 % of the lower velocity volume in the aquaculture tank

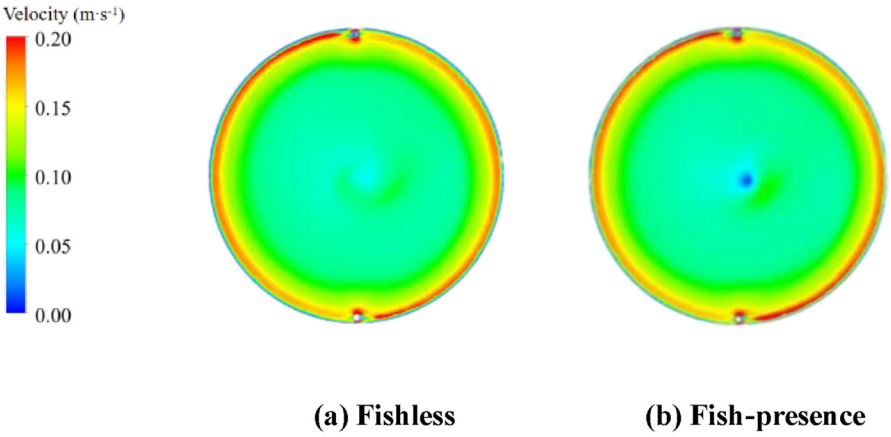

Fig. 9. The contour maps of velocity distribution in tanks.

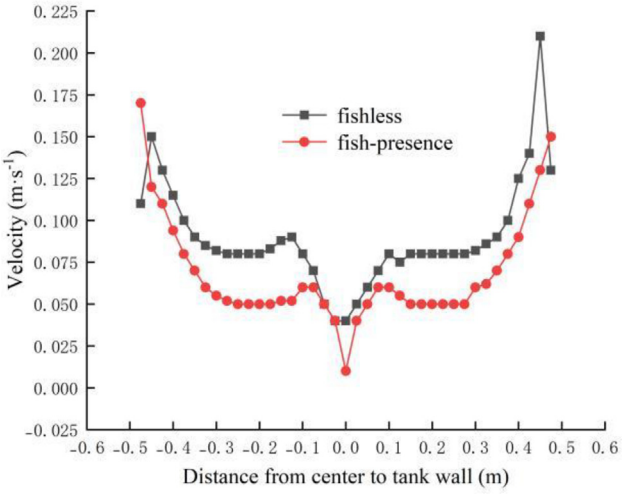

Fig. 10. Comparison of the velocity in the tank under two different working conditions.

(m/s); VH_{50} is the average value of velocity for 50 % of the higher velocity volume in the aquaculture tank (m/s).

$$DU_{50} = \frac{V_{50}}{V_1} \times 100 \tag{10}$$

where V_{50} is the average of 50 % of the lower velocities in the aquaculture tank (m/s); V_1 is the average velocity (m/s) of the plane being monitored, obtained by weighting the radii.

$$V_1 = \frac{\sum V_i r_i}{\sum r_i} \tag{11}$$

where V_i is the velocity (m/s) at a radial r_i position (m).

UC_{50} close to 1 or DU_{50} close to 100 means that the closer the average low flow velocity was to the average high flow velocity, the better the overall flow field homogeneity in the tank.

Tables 3 and 4 display the UC_{50} and DU_{50} values for the aquaculture tanks in two distinct operational scenarios: fish and unloaded aquaculture tanks. The results indicate that the presence of fish in the tanks significantly decreased UC_{50} and DU_{50} values, owing to the counter-current swimming behavior of the fish. Furthermore, this decrease becomes slightly more pronounced as the fish increases. Consequently, the flow field uniformity in the fish aquaculture tanks was reduced.

To investigate the effect of the counter-current motion of cultured fish on the flow field uniformity of the aquaculture tank, 100 fluid mass points were taken at the inlet of the aquaculture tank to draw the flow line diagram (Fig. 11). Figure 11 reveals that the flow line length in the fish culture tank was significantly shortened. The traveling distance and

Table 3. Influence of fish on UC_{50} under different working conditions.

Number of fish	UC_{50}	Rate of change
0 (No fish)	0.551	–
1	0.452	18.0 %
2	0.447	18.9 %
3	0.445	19.2 %
4	0.444	19.4 %
5	0.442	19.8 %

Table 4. Influence of fish on DC_{50} under different working conditions.

Number of fish	DU_{50}	Rate of change
0 (No fish)	71.0	–
1	62.6	11.8 %
2	61.8	13.0 %
3	61.6	13.2 %
4	61.5	13.4 %
5	61.3	13.7 %

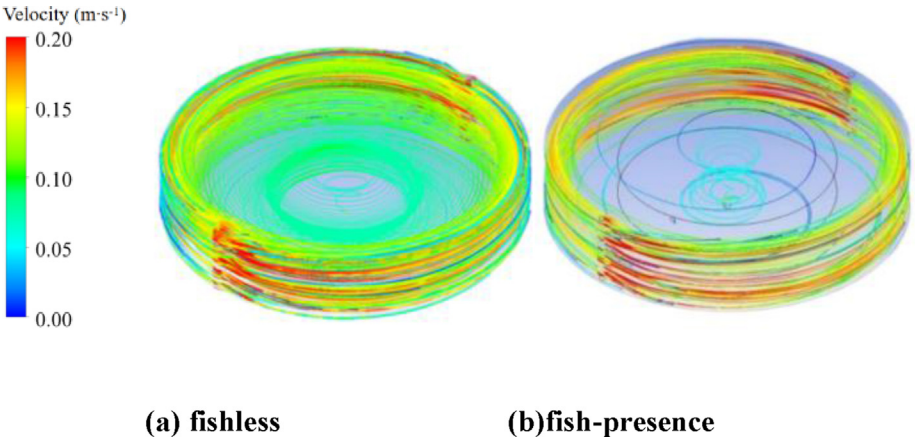

Fig. 11. 3D streamline diagram of aquaculture tank under two working conditions.

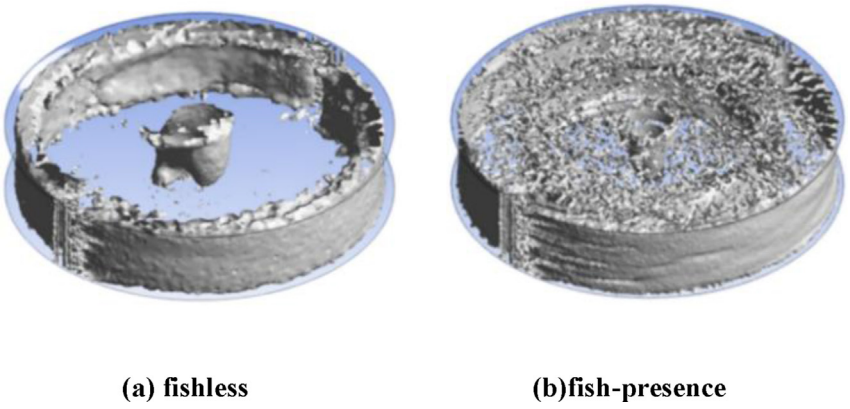

Fig. 12. 3D vorticity diagram of the flow field in the aquaculture tank under two working conditions.

movement speed of water mass points under this condition become shorter than the unloaded tank, consistent with the flow velocity in the fish culture tank, which becomes smaller in Section 3.1.

The Q criterion [27,28] was used to depict the distribution of vortex volume in the aquaculture tank, where the value of Q was 0.001. Figure 12 displays the vortex volume diagram, indicating that the volume of vortex columns was larger in the fishless unloaded aquaculture tanks, and the vortex ring distribution was regular. There are no stray vortex filaments and small vortex distribution in the tanks, and the uniformity of the water column in the tanks was good. The vortex column in the fish aquaculture tank was small in size, the shape of the vortex ring was insignificant, and the distribution was irregular in the tank wall. This was primarily attributed to the counter-current swimming of fish, increasing the vortex in the aquaculture tank. Consequently, the water body experienced a loss of energy and a decrease in homogeneity, thereby impacting the overall quality of the aquaculture tank.

4. Conclusions

Our study constructed an aquaculture tank model based on the MRF model, simulated the flow field of an aquaculture tank with cultured fish swimming, and compared it with the flow field of an aquaculture tank with no fish swimming, using redfin puffer as the simulated object of *T. rubripes*. The results revealed the following.

(1) When different numbers of fish swim against the current with fixed trajectories in the aquaculture tank, the overall average speed of the aquaculture tank significantly decreases under the influence of the counter-current movement of the fish. Moreover, the magnitude of the decrease slightly increased with the increase in the number of fish. When the same number of fish swim against the current with fixed trajectories, the influence of side-by-side distribution on the overall average flow rate of the aquaculture tank was slightly increased compared with the front-to-back and the top-to-bottom distributions.

(2) The counter-current movement of fish increased the flow velocity at the side walls of the tank, which was conducive to the scouring of walls by water. Simultaneously, a low-flow zone could appear near the tank center.
(3) Due to the counter-current swimming movement of fish, the movement trajectory of water quality points in the aquaculture tank became shorter. Furthermore, many small eddies were generated, reducing the flow field uniformity of the aquaculture tank.

Declaration of competing interest

The authors declare that they have no known competing financial interests or personal relationships that could have appeared to influence the work reported in this paper.

Acknowledgments

This research was financially supported by the Central Government Subsidy Project for Liaoning Fisheries(2023), the Innovation Support Program for High-level Talents of Dalian City (2019RD12) and the earmarked fund for CARS-49, Key research project of Liaoning Provincial Department of Education in 2022(LJKZZ20220091), The Opening Project of Key Laboratory of Environment Controlled Aquaculture (Dalian Ocean University), Ministry of Education (2021-MOEKLECA-KF-08 and 202312).

We thank Home for Researchers editorial team (www.home-for-researchers.com) for language editing service.

References

[1] Gu CC, Zhang YL. Overview of research progress on flow regimes in factory farmed fish tanks at home and abroad. Fish Modern 2013;40(6):10−4 [in Chinese)].
[2] Pan RH, Hu YC, Lu NJ, Li SD. Research progress of recirculating water aquaculture technology. Scientific Fish Farming 2018;11:1−2 (in Chinese).
[3] Huang CX, Liu YB, Li XC, Chen YR, Zhao FQ, Hou WX, et al. Fisheries engineering. Higher Education Press; 2009. p. 118−25 (in Chinese).
[4] Hu JC, Yu XQ, Xin NH, Xing KZ. Current status and application prospects of factory recirculating water aquaculture research. China Aquacult 2017;6:94−7 (in Chinese).
[5] Tang RX, Shi C, Liu Y. Investigation and analysis of the main problems in the 6. management and operation of recirculating water aquaculture systems. J Guangdong Ocean Univ 2018;38(1):100−6 (in Chinese).
[6] Tan CX. Effects of aquaculture density and feeding frequency on growth performance, body composition, digestive enzyme activity and serum biochemical indices of flower eels in recirculating water aquaculture mode. Shanghai Ocean University; 2016 (in Chinese).
[7] Chen F, Pan Y, Gui FK. Research on tubular jet drive for runway-type shrimp tanks. J Zhejiang Ocean Coll (Nat Sci Ed) 2017;36(3):207−11 (in Chinese).
[8] Masaló I, Oca J. Influence of fish swimming on the flow pattern of circular tanks. Aquacult Eng 2016;74:84−95.
[9] Masaló I, Reig L, Oca J. Study of fish swimming activity using acoustical Doppler velocimetry (ADV) techniques. Aquacult Eng 2008;38:43−51.
[10] Plew DR. Changes to flow and turbulence caused by different concentrations of fish in a circular tank. J Hydraul Res 2015;53:364−83.
[11] Liu HB, Zhou YX, Ren XZ, Liu SS, Liu HF, Li M. Numerical modeling and application of the effects of fish movement on flow field in recirculating aquaculture system. Ocean Eng 2023;285:115432.
[12] Gorle JMR, Terjesen BF, Mota VC, Summerfelt S. Water velocity in commercial RAS aquaculture tanks for Atlantic salmon smolt production. Aquacult Eng 2018;81:89−100.
[13] Gorle JMR, Terjesen BF, Summerfelt ST. Hydrodynamics of octagonal aquaculture tanks with Cornell-type dual-drain system. Comput Electron Agric 2018;151:354−64.
[14] Zhang SH, Yu GH, Wang Y, Li DL, Li WS. Numerical investigations on temperature and flow field performance of octagonal culture tank under different physical parameters for fish growth based on computational fluid dynamics. Comput Electron Agric 2022;195:106821.
[15] Behroozi L, Couturier MF. Prediction of water velocities in circular aquaculture tanks using an axisymmetric CFD model. Aquacult Eng 2019;85:114−28.
[16] Zhang SH, Yu GH, Guo Y, Wang Y. Modelling development and optimization on hydrodynamics and energy utilization of fish culture tank based on computational fluid dynamics and machine learning. Energy 2023;276:127518.
[17] Boris Miguel López-Rebollar, García-Pulido Daury, Diaz-Delgado Carlos, Gallego-Alarcón Ivan, Juan Antonio García-Aragón, Salinas-Tapia Humberto. Sedimentation efficiency evaluation of an aquaculture tank through experimental floc characterization and CFD simulation. I. 2023. p. 102343. Vol. 102.
[18] Lunger A, Rasmussen MR, Laursen Jesper, McLean Ewen. Fish stocking density impacts tank hydrodynamics. Aquaculture 2006;254:370−5.
[19] Liu NS, Liu S, Yu GY. Numerical simulation and study of hydrodynamic characteristics of two types of dual-channel circular aquaculture tanks. Fish Modern 2017;44(No.003):1−6 (in Chinese).
[20] An CH, Sin MG, Kim MJ, Jong IB, Song GJ, Choe C. Effect of bottom drain positions on circular tank hydraulics: CFD simulations. Aquacult Eng 2018;83:138−50.
[21] Liu HB, Ren XZ, Zhang Q, Bi CW. Numerical modeling of fish movement in recirculating water aquaculture tanks: the case of *Sebastes schlegelii*. J Dalian Ocean Univ 2021;36(6): 995−1002 (in Chinese).
[22] Liu Y, Liu BL, Lei JL. Numerical simulation of the hydrodynamics within octagonal tanks in recirculating aquaculture systems. Chin J Oceanol Limnol 2017;35(No.04):912−20 (in Chinese).
[23] Dong M, Xia CL, Li X. Numerical simulation of internal flow field in combined paddle stirred tank. J Drain Irrig Mach Eng 2018;36(No.012):1288−93 (in Chinese).
[24] Ren XZ, Zhang Q, Jiang HZ, Gui JS, Bi CW. Structural optimization of ingle-channel square mariculture tanks based on flow field uniformity. Mar Environ Sci 2021; 40(No.02):287−93 (in Chinese).
[25] Xue BR, Yu LP, Zhang Q, Ren XZ, Bi CW. Influence of feed-to-diameter ratio on hydrodynamic characteristics of rectangular rounded-angle aquaculture tanks. J Aquacult 2021; 45(3):444−52 (in Chinese).
[26] Oca J, Masaló I. Influence of fish swimming on the flow pattern of circular tanks. Aquacult Eng 2016;74.
[27] Dong XR, Wang YQ, Chen XP, Dong YL, Zhang YN, Liu CQ. Determination of epsilon for Omega vortex identification method. J Hydrodyn 2018;30(No. 4):541−8.
[28] Chakraborty P, Balachandar S, Adrian RJ. On the relationships between local vortex identification schemes. J Fluid Mech 2005;535:189−214.